Biochemistry

 Volume 28, Number 5 March 7, 1989

Perspectives in Biochemistry

Human Leukocyte and Porcine Pancreatic Elastase: X-ray Crystal Structures, Mechanism, Substrate Specificity, and Mechanism-Based Inhibitors[†,‡]

Wolfram Bode,[§] Edgar Meyer, Jr.,[∥] and James C. Powers*

Max-Planck-Institut für Biochemie, D-8033 Martinsried, West Germany, Department of Biochemistry, Texas A&M University, College Station, Texas 77843, and School of Chemistry, Georgia Institute of Technology, Atlanta, Georgia 30332

Received November 2, 1988; Revised Manuscript Received December 19, 1988

The serine protease family of enzymes is one of the most widely studied group of enzymes, as evidenced by the fact that more crystal structures are available for individuals of this superfamily than for any other homologous group of enzymes. These enzymes contain a conserved triad of catalytic residues including Ser-195, His-57, and Asp-102. The active-site serine is very nucleophilic, and serine proteases are inhibited by specific serine protease reagents such as diisopropyl phosphorofluoridate (DFP), phenylmethanesulfonyl fluoride, and 3,4-dichloroisocoumarin (Harper et al., 1985). The structure, chemistry, and biochemistry of serine proteases are discussed in recent reviews (Bieth, 1986; Bode & Huber, 1986; Kraut, 1977; Neurath, 1986; Powers & Harper, 1986).

Elastases are a group of proteases that possess the ability to cleave the important connective tissue protein elastin (Bieth, 1986; Werb et al., 1982). Elastin has the unique property of elastic recoil, is widely distributed in vertebrate tissue, and is particularly abundant in the lungs, arteries, skin, and ligaments. This flexible protein is highly cross-linked with unusual amino acid residues such as desmosine and isodesmosine, which contain pyridinium rings, it is rich in amino acids with small side chains (Ala, Ser, Val) and is poor in aromatic or basic amino acids. A wide variety of proteases possess the ability to cleave elastin including thiol proteases such as papain, metalloproteases such as *Pseudomonas aeruginosa* elastase and related enzymes secreted from a variety of virulent pathogenic organisms (e.g., *Schistosoma mansoni*), and many important serine proteases.

Human neutrophil elastase and pancreatic elastase are two major serine proteases that cleave elastin. Neutrophil elastase is found in the dense granules of polymorphonuclear leukocytes and is essential for phagocytosis and defense against infection by invading microorganisms. Pancreatic elastase is stored as an inactive zymogen in the pancreas and is secreted into the intestines where it becomes activated by trypsin and then participates in digestion. Both elastases cleave substrates at peptide bonds where the P_1 residue is an amino acid residue with a small alkyl side chain.[1] Although PP[2] and HL elastase cleave elastin, elastin is neither their only substrate nor necessarily their most important physiological substrate. In particular, the powerful proteolytic activity of neutrophil elastase is essential for migration of neutrophils through connective tissue and for the destruction of foreign bacterial invaders which do not contain elastin.

Elastases can be extremely destructive if not controlled because they can destroy many connective tissue proteins. Under normal physiological conditions these proteases are carefully regulated by compartmentalization or by natural circulating plasma protease inhibitors. Any elastase that reaches the circulation is quickly complexed by the natural inhibitors α_1-protease inhibitor (α_1-antitrypsin) and α_2-

[†] Supported by grants from the Deutsche Forschungsgemeinschaft to W.B. (SFB 207/H-1), from the Robert A. Welch Foundation (A328) to E.M., and from the National Institutes of Health to J.C.P. (HL29307 and HL34035).

[‡] This perspective is dedicated to the memory of Aaron Janoff, who did so much to elucidate the biological function of human leukocyte elastase.

* Address correspondence to this author at Georgia Institute of Technology.

[§] Max-Planck-Institut für Biochemie.

[∥] Texas A&M University.

[1] The nomenclature of Schechter and Berger (1967) is used to designate the individual amino acid residues (P_2, P_1, P_1', P_2', etc.) of a peptide substrate and the corresponding subsites (S_2, S_1, S_1', S_2', etc.) of the enzyme. The scissile bond is the P_1–P_1' peptide bond. Amino acid residues of the turkey ovomucoid inhibitor third domain (TOM) residues are labeled with I.

[2] Abbreviations: Ahe, 2-aminohexanoic acid (Nle, norleucine); Ape, 2-aminopentanoic acid (Nva, norvaline); HL, human leukocyte; HLE, human leukocyte (neutrophil) elastase; MeLeu, *N*-methylleucine; MeO-Suc, methoxysuccinyl; PP, porcine pancreatic; PPE, porcine pancreatic elastase; rms, root mean square; Boc, *tert*-butyloxycarbonyl; TOM, turkey ovomucoid inhibitor third domain; Tos, *p*-toluenesulfonyl.

0006-2960/89/0428-1951$01.50/0

Table I: Sequence Alignment of Human Leukocyte Elastase (HLE) and Porcine Pancreatic Elastase (PPE) Based on Topological Criteria[a]

	16	17	18	19	20	21	22	23	24	25	26	27	28	29	30
HLE	ILE	VAL	GLY	GLY	ARG	ARG	ALA	ARG	PRO	HIS	ALA	TRP	PRO	PHE	MET
PPE	VAL	VAL	GLY	GLY	THR	GLU	ALA	GLN	ARG	ASN	SER	TRP	PRO	SER	GLN

	31	32	33	34	35	36	36A	36B	36C	37	38	39	40	41	42
HLE	VAL	SER	LEU	GLN	LEU	ARG	-	-	-	-	GLY	GLY	HIS	PHE	CYS
PPE	ILE	SER	LEU	GLN	TYR	ARG	SER	GLY	SER	SER	TRP	ALA	HIS	THR	CYS

	43	44	45	46	47	48	49	50	51	52	53	54	55	56	57
HLE	GLY	ALA	THR	LEU	ILE	ALA	PRO	ASN	PHE	VAL	MET	SER	ALA	ALA	HIS
PPE	GLY	GLY	THR	LEU	ILE	ARG	GLN	ASN	TRP	VAL	MET	THR	ALA	ALA	HIS

	58	59	60	61	62	63	63A	63B	63C	64	65	65A	66	67	68
HLE	CYS	VAL	ALA	ASN	VAL	ASN	VAL	ARG	ALA	VAL	ARG	-	VAL	VAL	LEU
PPE	CYS	VAL	ASP	ARG	GLU	LEU	-	-	-	THR	PHE	ARG	VAL	VAL	VAL

	69	70	71	72	73	74	75	76	77	78	79	80	81	82	83
HLE	GLY	ALA	HIS	ASN	LEU	SER	ARG	ARG	GLU	PRO	THR	ARG	GLN	VAL	PHE
PPE	GLY	GLU	HIS	ASN	LEU	ASN	GLN	ASN	ASN	GLY	THR	GLU	GLN	TYR	VAL

	84	85	86	87	88	89	90	91	92	93	94	95	96	97	99
HLE	ALA	VAL	GLN	ARG	ILE	PHE	GLU	-	ASN	GLY	TYR	ASP	PRO	VAL	ASN
PPE	GLY	VAL	GLN	LYS	ILE	VAL	VAL	HIS	PRO	TYR	TRP	ASN	THR	ASP	ASP

	99A	99B	100	101	102	103	104	105	106	107	108	109	110	111	112
HLE	-	-	LEU	ASN	ASP	ILE	VAL	ILE	LEU	GLN	LEU	ASN	GLY	SER	ALA
PPE	ALA	ALA	GLY	TYR	ASP	ILE	ALA	LEU	LEU	ARG	LEU	ALA	GLN	SER	VAL

	113	114	115	116	117	118	119	120	121	122	123	124	125	126	127
HLE	THR	ILE	ASN	ALA	ASN	VAL	GLN	VAL	ALA	GLN	LEU	PRO	ALA	GLN	GLY
PPE	THR	LEU	ASN	SER	TYR	VAL	GLN	LEU	GLY	VAL	LEU	PRO	ARG	ALA	GLY

	128	129	130	131	132	133	134	135	136	137	138	139	140	141	142
HLE	ARG	ARG	LEU	GLY	ASN	GLY	VAL	GLN	CYS	LEU	ALA	MET	GLY	TRP	GLY
PPE	THR	ILE	LEU	ALA	ASN	ASN	SER	PRO	CYS	TYR	ILE	THR	GLY	TRP	GLY

	143	144	145	146	147	148	150	151	152	153	154	155	156	157	158
HLE	LEU	LEU	GLY	ARG	ASN	ARG	GLY	ILE	ALA	SER	VAL	LEU	GLN	GLU	LEU
PPE	LEU	THR	ARG	THR	ASN	GLY	GLN	LEU	ALA	GLN	THR	LEU	GLN	GLN	ALA

	159	160	161	162	163	164	165	166	167	168	169	170	170A	170B	171
HLE	ASN	VAL	THR	VAL	VAL	THR	SER	LEU	-	CYS	-	-	-	-	-
PPE	TYR	LEU	PRO	THR	VAL	ASP	TYR	ALA	ILE	CYS	SER	SER	SER	SER	TYR

	172	173	174	175	176	177	178	179	180	181	182	183	184	185	186
HLE	-	-	-	-	-	ARG	ARG	SER	ASN	VAL	CYS	THR	LEU	VAL	ARG
PPE	TRP	GLY	SER	THR	VAL	LYS	ASN	SER	MET	VAL	CYS	ALA	GLY	GLY	ASP

	186A	186B	187	188	188A	189	190	191	192	193	194	195	196	197	198
HLE	GLY	ARG	GLN	ALA	-	GLY	VAL	CYS	PHE	GLY	ASP	SER	GLY	SER	PRO
PPE	-	-	GLY	VAL	ARG	SER	GLY	CYS	GLN	GLY	ASP	SER	GLY	GLY	PRO

	199	200	201	202	203	204	205	206	207	208	209	210	211	212	213
HLE	LEU	VAL	CYS	ASN	-	-	-	-	GLY	LEU	ILE	HIS	GLY	ILE	ALA
PPE	LEU	HIS	CYS	LEU	VAL	ASN	GLY	GLN	TYR	ALA	VAL	HIS	GLY	VAL	THR

	214	215	216	217	217A	218	219	220	220A	221	222	223	224	225	226
HLE	SER	PHE	VAL	ARG	-	GLY	GLY	CYS	ALA	SER	GLY	LEU	TYR	PRO	ASP
PPE	SER	PHE	VAL	SER	ARG	LEU	GLY	CYS	ASN	VAL	THR	ARG	LYS	PRO	THR

	227	228	229	230	231	232	233	234	235	236	237	238	239	240	241
HLE	ALA	PHE	ALA	PRO	VAL	ALA	GLN	PHE	VAL	ASN	TRP	ILE	ASP	SER	ILE
PPE	VAL	PHE	THR	ARG	VAL	SER	ALA	TYR	ILE	SER	TRP	ILE	ASN	ASN	VAL

	242	243	244	245
HLE	ILE	GLN	-	-
PPE	ILE	ALA	SER	ASN

[a] Chymotrypsinogen numbering.

macroglobulin. The complexes are cleared from the plasma by the liver and/or macrophages and are degraded. When an imbalance occurs due to a deficiency of effective α_1-protease inhibitor or abnormally high levels of elastases, severe permanent tissue damage may occur. Pancreatic elastase participates in the usually fatal disease pancreatitis, which occurs when pancreatic zymogens are activated and released into the circulation. Neutrophil elastase has been linked to pulmonary emphysema, acute respiratory distress syndrome, shocked lung, glomerulonephritis, rheumatoid arthritis, and other inflammatory disorders.

Elastase Structures

Sequences. The primary structures of porcine pancreatic elastase (PPE) and human leukocyte elastase (HLE) are shown in Table I. The alignment is based on tertiary structure similarities and follows the common practice of using the bovine chymotrypsinogen A numbering (Hartley, 1964). PPE is a single peptide chain of 240 amino acids beginning with Val-16 and terminating with Asn-245. It contains four disulfide bridges and no carbohydrate (Shotton & Hartley, 1970).

The sequence of HLE was established by a combination of peptide sequencing (Sinha et al., 1987) and crystallographic methods (Bode et al., 1986b). HLE is a glycoprotein with a single peptide chain of 218 amino acid residues and four disulfide bridges. Analyses of the cDNA sequence of HLE (Farley et al., 1988; Takahashi et al., 1988a) confirmed the sequence with the addition of a carboxy-terminal 20 amino acid extension. The extension is probably removed during posttranslational trimming and packaging in the lysosomal granules. Medullasin, an inflammatory serine proteinase derived from bone marrow cells, is similar to if not identical with HLE (Aoki, 1978; Okano et al., 1987).

HLE is homologous with other elastolytic serine proteases such as PPE (40%), rat pancreatic elastase II (40%; MacDonald et al., 1982), human pancreatic elastase I (37%; Tani et al., 1988), and human pancreatic elastase E (36%; Shen et al., 1987). The sequence identity with less related proteases such as rat mast cell protease II (Woodbury et al., 1978), porcine pancreatic kallikrein (Bode et al., 1983), rat tonin (Fujinaga & James, 1987), bovine chymotrypsin (Cohen et al., 1981; Tsukuda & Blow, 1985), human cathepsin G, human lymphocyte proteases, and human plasminogen is ca. 32–35%. PPE exhibits the same degree of sequence identity with bovine pancreatic chymotrypsin (39%) and trypsin (37%), but the identity is much higher with functionally related mammalian pancreatic elastases including human elastase I (90%), human protease E (57%), rat elastase I (85%; MacDonald et al., 1982), and rat elastase II.

HLE and PPE: Tertiary Structures. Crystal structures of 19 or more elastase derivatives have been determined to atomic resolution (Table II). PPE (as the tosyl derivative) was the second serine protease whose tertiary structure was elucidated (Watson et al., 1970; Shotton & Watson, 1970; Sawyer et al., 1978), and the structure of native elastase has recently been refined crystallographically to 1.65-Å resolution (Meyer et al., 1988a). Native HLE produces small crystals unsuitable for analysis (E. F. Meyer and W. Bode, unpublished results), but the structures of two separate HLE–inhibitor complexes have been determined (Bode et al., 1986b; Wei et al., 1988). The structure analyses of two more complexes of HLE with protein protease inhibitors are nearly complete, but attempts to cocrystallize HLE with other small ligands have been unsuccessful up to now. Fortunately, unligated PPE yields beautiful single crystals with a binding site that is relatively open and accessible to low molecular weight substrate analogues and inhibitors except at remote subsites. Small inhibitors can readily be soaked into the crystals, and the crystal structures of several PPE complexes formed with various peptidic and heterocyclic inhibitors have been analyzed (Table II). All the PPE structures have been based on the same isomorphous crystal form while the HLE complexes exhibit different crystal packing arrangements.

Along with other serine proteases, the polypeptide chains of PPE and HLE are organized as two structurally similar, interacting antiparallel β-barrel cylindrical domains. Only an intermediate segment and the carboxy-terminal segment are organized as helices (Figure 1). Most of the catalytic residues, especially those of the active-site triad Ser-195, His-57, and Asp-102, are localized in the crevice formed between both domains. Across this crevice is the substrate binding site, which includes parts of both domains.

Of all the serine proteases whose tertiary structures have been determined, PPE is topologically most similar to HLE,

Table II: Human Leukocyte Elastase and Porcine Pancreatic Elastase Crystal Structures

structure	resoln (Å)	R-factor (%)	reference
Human Leukocyte Elastase Complexes			
turkey ovomucoid inhibitor third domain (TOM)	1.80	16.7	Bode et al., 1986b
MeO-Suc-Ala-Ala-Pro-Val-CH_2Cl	2.30	14.5	Wei et al., 1988
MeO-Suc-Ala-Ala-Pro-Ala-CH_2Cl	1.84	16.4	Navia et al., 1989
Porcine Pancreatic Elastase Structures			
tosyl elastase	2.50	32.6	Sawyer et al., 1978
native (70% methanol buffer)	1.65	16.6	Meyer et al., 1988a
CF_3CO-Lys-Ala-NH-C_6H_4-CF_3	2.50	21	Hughes et al., 1982
CH_3CH_2CO-Ala-Pro-NH-Et (and -NH-C_5H_9)	3.50		Hassal et al., 1979
Ac-Ala-Pro-Ala (pH 5.0)	1.65	18.4	Meyer et al., 1986
Ac-Ala-Pro-Ala (pH 7.5)	1.65	18.6	unpublished results
Ac-Pro-Ala-Pro-Tyr	1.80	19.2	Clore et al., 1986
Thr-Pro-Ape*MeLeu-Tyr-Thr[a]	1.80	18.8	Meyer et al., 1988b
Ac-Ala-Pro-Val-CF_3	2.50	15.0	Takahashi et al., 1988b
Ac-Ala-Pro-Val-CF_2CO-NH-$CH_2CH_2C_6H_5$	1.78	16.0	Takahashi et al., 1989
5-Me-2-[Boc-NHCH(*i*-Pr)]benzoxazinone	2.10	15.3	Radhakrishnan et al., 1987
5-Cl-2-[Boc-NHCH(*i*-Pr)]benzoxazinone	1.74	17.2	Radhakrichnan et al., 1987
7-amino-4-chloro-3-methoxyisocoumarin	1.80	17.5	Meyer et al., 1985
4-chloro-3-ethoxy-7-guanidinoisocoumarin	1.70	21.0	E. F. Meyer and R. Radhakrishnan, unpublished results
cephalosporin derivative	1.84	16.8	Navia et al., 1987

[a] The asterisk indicates the peptide bond corresponding to the scissile bond of a good substrate.

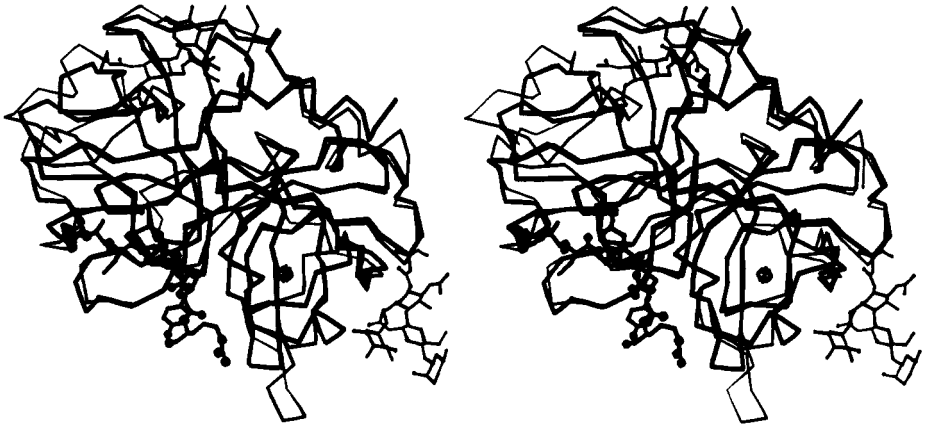

FIGURE 1: Stereoview of the α-carbon backbone of HLE (dark lines) superimposed onto that of PPE (thin lines). The two carbohydrate moieties of HLE are included together with their points of attachment (Asn-159 and Asn-109). The calcium atom bound to PPE is drawn as a ball; this site is occupied by Arg-80 in HLE. The primary binding segment of TOM is shown (with heteroatoms drawn as small spheres) in order to indicate the substrate binding site.

followed by rat mast cell protease II (Remington et al., 1988), porcine pancreatic kallikrein (Bode et al., 1983), rat tonin (Fujinaga & James, 1987), and bovine chymotrypsin (Cohen et al., 1988; Tsukuda & Blow, 1985). Most of the structural differences between the elastases and other serine proteases are located in surface loops. PPE and HLE have approximately 150 equivalent α-carbon atoms at a rms deviation of 0.6 Å (W. Bode, unpublished results). The topological alignment of PPE and HLE is shown in Table I; a similar alignment of HLE and α-chymotrypsin has been reported (Wei et al., 1988).

The two elastases are surprisingly similar especially in their active-site regions. The catalytic triad (Ser-195, His-57, and Asp-102) and the residues forming the central core of the binding site (i.e., peptide segments 189 to Ser-195, 213–216, 226–228, residue 41) are structurally similar, with their α-carbon atoms exhibiting a rms deviation of only 0.35 Å. When the backbone atoms of these residues are superimposed, 55 atoms agree to 0.26 Å, the greatest divergence occurring at amino acids 192 and 226.

There are significant structural differences between the two elastases that include 10 deletions (comprising 27 residues) and 2 insertions (comprising 5 residues). In addition, larger spatial deviations between the peptide chains occur at amino acid residues 25, 75–79, 88, 130–133, 147–150, 177–180, and 240–243. The largest structural differences are observed around the "methionine loop" (centered around Met-180 in PPE and α-chymotrypsin; Asn in HLE). In addition, one of the four disulfide bridges (Cys-168–Cys-182) is of quite different size and has a different conformation due to a long deletion in HLE. There is no indication in HLE of an intermediate helix which is normally observed around Cys-168 in other vertebrate proteases including PPE. The other three disulfide bridges (42–58, 136–201, and 191–220) are geometrically similar in both elastases.

PPE and the other digestive enzymes trypsin (Bode & Schwager, 1975) and α-chymotrypsin (Birktoft & Blow, 1972) possess a calcium binding loop composed of the peptide segment Glu-70–Glu-80 with the Glu residues acting as ligands. Binding of calcium to this loop stabilizes the molecule but does not affect its catalytic activity (Bode & Schwager, 1975). The equivalent peptide segment in HLE is spatially similar to the calcium loop in PPE and trypsin; however, Glu-80 (PPE and trypsin) is replaced by Arg-80 in HLE. The terminal guanidino group of Arg-80 in HLE occupies the site where calcium is found in PPE and trypsin. Thus HLE carries its own stabilizing cation and does not depend on calcium for stability.

Both PPE and HLE contain several internal or "buried"

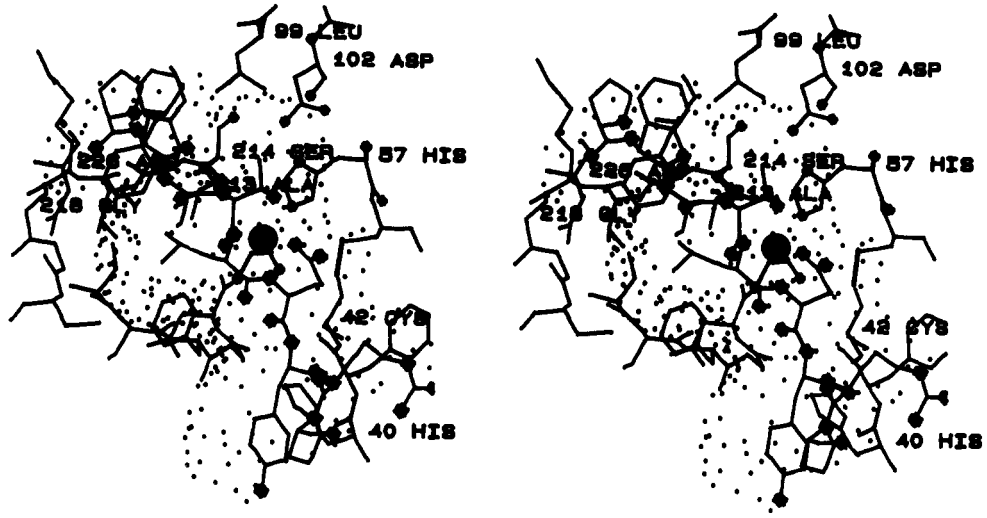

FIGURE 2: Stereoview of the binding of the octapeptide strand (14I–22I) of TOM to the extended substrate binding site of HLE. For the sake of discrimination, heteroatoms in the inhibitor segment are drawn as large spheres and those in the catalytic triad as small spheres. A double van der Waals' contact surface illustrates the structurally convoluted extended binding site of HLE. Ser-195 Oγ is drawn as an enlarged sphere for the purposes of orientation.

channels or domains of water that are common to other serine proteases. The seven water domains in PPE (Meyer et al., 1988a) are present in HLE, even though the enzymes have considerable sequence and structural differences in the immediate vicinity of the water domains. The presence of a channel of water linking the buried portion of the catalytic triad to the surface of the enzyme is especially noteworthy. The presence of similar water channels in other hydrolases suggests that this channel may have a functional role (E. F. Meyer, unpublished observations).

HLE is much more hydrophobic and at the same time more basic than PPE. In HLE approximately 90 hydrophobic residues (>40% of its total residues) are accessible to bulk water molecules, compared to only 70 such residues (30%) in PPE. HLE owes its high basicity to the presence of 19 arginines, which are balanced with only 9 acidic residues (three of which, Asp-102, Asp-194, and Asp-226, are buried). All of the arginine residues, with the exception of Arg-80, are arranged on the surface of the enzyme in a horseshoe-like manner around the active site, with several forming clusters of two to four arginines. The surface arrangement of arginines around the active site explains the preferred binding of linear sulfated polysaccharides to HLE (Baici et al., 1980).

HLE along with many other human serine proteases such as the human pancreatic protease E (I. A. Szigoleit, personal communication) is a glycoprotein, while PPE is devoid of prosthetic groups. Two of HLE's three Asn-X-Ser/Thr consensus glycosylation sequences (Asn-109 and Asn-159) are linked to different degrees with carbohydrate chains (Figure 1; Bode et al., 1986b; Sinha et al., 1987), giving rise to three isoenzyme forms of HLE (E1, E2, and E3) with almost identical enzymatic activity (Baugh & Travis, 1976). Only the first three to four sugar residues at both glycosylation sites are defined by proper electron density and have a rigid relationship to the polypeptide backbone in the crystalline complex. Most of the noncovalent contacts between the polysaccharide and the peptide backbone are formed with the fucose ring. Both sugar chains extend out into solution and are located away from the substrate binding site. Consequently, they should not interfere with binding of substrates and inhibitors at the active site. However, the carbohydrate chains affect crystallization. Different HLE isoenzyme forms, when crystallized with TOM, crystallize under different conditions (W. Bode, W. Watorek, and J. Travis, unpublished results). The carbohydrate structure in the HLE–TOM complex is probably the best defined of any glycoprotein now available at high resolution.

Peptide Inhibitors and the Extended Substrate Binding Site

HLE–TOM Complex. HLE is inhibited by several naturally occurring or engineered protein protease inhibitors including the following: α_1-protease inhibitor (Travis & Salvesen, 1983) and some genetically engineered variants (Rosenberg et al., 1984); eglin c (Baici & Seemueller, 1984; Bode et al., 1986a; Braun et al., 1987); bovine pancreatic trypsin inhibitor and some variants (Tschesche et al., 1988); ovomucoid inhibitors and inhibitors derived from the human pancreatic trypsin inhibitor; human seminal plasma inhibitor/human secretory leukocyte inhibitor/human mucous protease inhibitor (Seemueller et al., 1986; Thompson & Ohlsson, 1986; Gruetter et al., 1988). Most protein protease inhibitors bind to their cognate serine proteases in the manner of a good substrate and form extremely stable Michaelis complexes in which the inhibitor's reactive-site peptide bond remains intact or is only cleaved extremely slowly (Huber & Bode, 1978; Laskowski & Kato, 1980; Marquart et al., 1983). Reactive-site loops of the inhibitors are complementary to the substrate recognition site of the cognate serine proteases, and thus these complexes are ideal for probing substrate binding subsites due to extensive interactions and tight binding between the enzyme and inhibitor.

The first structure of HLE was determined as a complex with the third domain of the turkey ovomucoid inhibitor (TOM). TOM forms tight complexes with both HLE and PPE with association constants of 6.2×10^9 M^{-1} and 4.1×10^{10} M^{-1}, respectively (M. Laskowski, S. J. Parks, M. Tashiro, and R. Wynn, personal communication). This inhibitor, like other Kazal-type inhibitors (Laskowski & Kato, 1980), consists of a molecular scaffold made up of an α-helical segment, a three-stranded β-pleated sheet, and an extended protease binding loop centered around the reactive-site scissile peptide bond Leu-18I–Glu-19I (Papamokos et al., 1982). The HLE binding site makes direct contact with eight residues of the "primary binding segment" (P_5 Pro-14I to P_3' Arg-21I) of TOM (Figure 2) and with an additional three (to five) residues (Gly-32I, Asn-33I, and Asn-36I) of a "secondary binding segment". The majority of the total intermolecular contacts

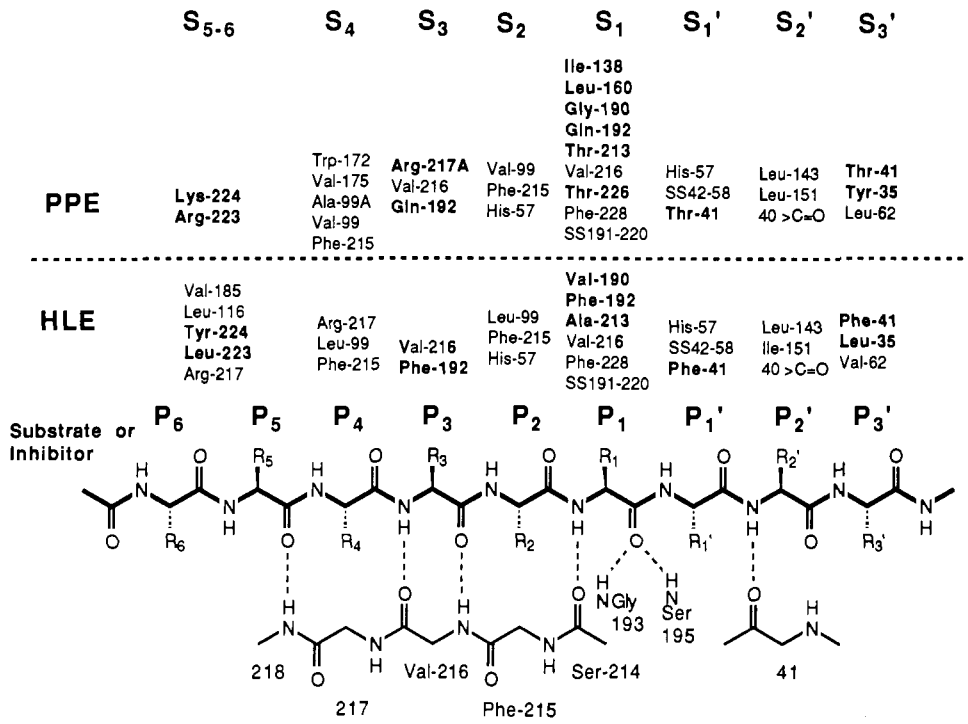

FIGURE 3: Schematic representation of the main-chain and side-chain interactions between the primary binding segment of TOM or a peptide substrate with HLE and PPE. Significant amino acid sequence changes that might influence specificity are shown in bold type. The subsites of the elastases are represented by S_1, S_1', etc. and the residues of the peptide by P_1, P_1', etc. The carbonyl of the scissile peptide bond is shown interacting with the oxyanion hole (hydrogen bonds to the backbone NHs of Gly-193 and Ser-195).

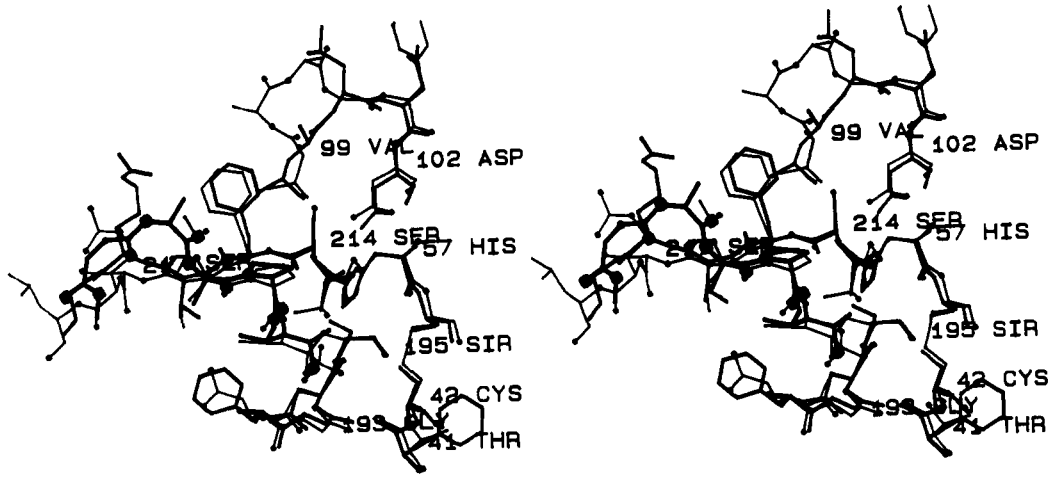

FIGURE 4: Comparison of the binding of peptide halo ketone inhibitors to HLE and PPE showing the similarity of binding modes. The complex of HLE with MeO-Suc-Ala-Ala-Pro-Val-CH_2Cl is drawn with heavy lines, while the PPE complex with Ac-Ala-Pro-Val-CF_3 is drawn with thin lines. Large and small spheres, respectively, indicate heteroatoms, including the fluorines of the fluoro ketone. The bonds between Ser-195 and His-57 of HLE and the chloro ketone are not shown. Significant differences in the two active sites (HLE vs PPE) are seen at residues 41 (Phe vs Thr) and 192 (Phe vs Gln). The 99A–99B insertion loop of PPE is shown at the top. Arg-217A, an insertion residue in PPE, is drawn on the left side of the figure in collision with the N-terminal methoxysuccinyl group of the chloromethyl ketone inhibitor of HLE.

(94 out of 106 contacts within 4 Å) involve the primary binding loop, which mimics a bound substrate. Seven hydrogen bonds are formed between the peptide backbones of the inhibitor segment and HLE (Figure 3). The P_3, P_2, and P_1 residues of the inhibitor form an antiparallel β-sheet structure with the peptide backbone of Ser-214–Val-216 of HLE, an interaction that is typical for the binding of peptides to serine proteases. The carbonyl group of Leu-18I is located in the oxyanion hole (Gly-193N, Ser-195N), and the P_2' residue makes an antiparallel arrangement with the backbone of Phe-41.

Complex of HLE and MeO-Suc-Ala-Ala-Pro-Val-CH_2Cl. The complex formed between HLE and the specific chloromethyl ketone irreversible inhibitor MeO-Suc-Ala-Ala-Pro-Val-CH_2Cl (Powers et al., 1977) was crystallized and its structure (Figure 4) determined by Patterson methods (Wei et al., 1988) (Table II). A similar structure of HLE inhibited by MeO-Suc-Ala-Ala-Pro-Ala-CH_2Cl will be available shortly (Navia et al., 1989; Williams et al., 1987). The inhibitor peptide chains of both chloromethyl ketones are bound in a conformation that is similar to the corresponding P_4 to P_1 residues of TOM. The MeO-Suc group (formally the P_5 group) of the valyl chloromethyl ketone is not rigidly fixed, but runs antiparallel to the backbone residues 216–218. In solution this group could be placed close to Arg-217, and a negatively charged succinyl group on an inhibitor could interact with the guanidino group of Arg-217.

Complexes of Peptides with PPE. The relatively open active site of crystalline PPE at S_3 to S_4' has facilitated isomorphous

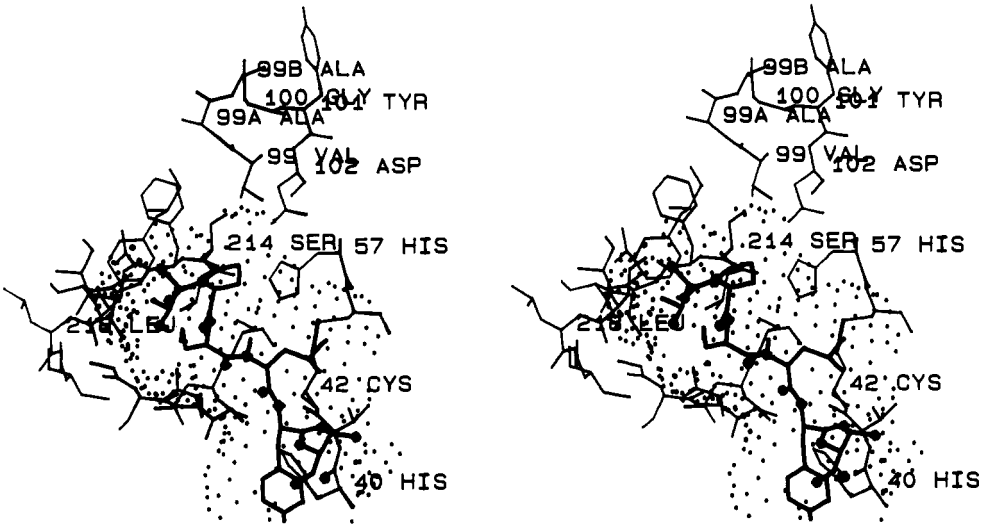

FIGURE 5: Stereoview of the extended binding site of PPE complexed with the hexapeptide Thr-Pro-Ape*MeLeu-Tyr-Thr (the asterisk indicates the peptide bond that corresponds to the scissile bond of a substrate). One of the insertion loops in PPE (99A–99B) is shown at the top of the figure.

crystallographic studies of the binding of peptides to this enzyme. However, remote subsites such as S_4 are blocked in crystals of PPE by Glu-62 from a symmetry-related neighbor. Low-resolution structures of PPE complexes with the dipeptides CH_3CH_2CO-Ala-Pro-NH-Et (or -NH-C_5H_9) first showed that peptides were binding to PPE in the vicinity of residues 214–216 (Hassal et al., 1979). Interestingly, the first peptide that was investigated at high resolution was found to bind backward in the active site of PPE, although this was not recognized at the time (Hughes et al., 1982). In this complex of PPE and CF_3CO-Lys-Ala-NH-C_6H_4-*p*-CF_3, the CF_3 group of the trifluoroacetyl group occupies the S_1 subsite and the peptide chain makes a parallel β-sheet structure with Ser-214–Phe-215–Val-216 instead of the more typical antiparallel β-sheet juxtaposition.

A number of peptides containing P_2 prolyl residues have been investigated at high resolution. While Pro at P_2 is not a prerequisite for binding, it eliminates (or reduces) the possibility of multiple binding in longer peptides and thus has been included in the design strategy of a number of ligands and substrates for PPE. This strategy does not always apply for short peptides; Ac-Pro-Ala-Pro-Tyr-NH_2 (Clore et al., 1986) binds on the S′ side of the active site, while two molecules of Ac-Ala-Pro-Ala (Meyer et al., 1986) bind backward on both the S and S′ sides of the binding site. Directed hydrogen bonds between the substrate peptide backbone atoms and PPE have a greater influence on binding architecture than do the side chains, which frequently point out into solution. This regular spacing of backbone interactions, especially on the acyl side of the scissile bond (S_1–S_3), permits the inverse binding that is observed with both peptides. Backward binding is also characterized by a translational half-step shift with respect to PPE's extended substrate binding site to enable formation of hydrogen bonds when a peptide is bound in the reverse orientation.

The structure of the complex of PPE with the hexapeptide Thr-Pro-Ape*MeLeu-Tyr-Thr (Figure 5) was the first PPE structure that showed the nature of subsites on both sides of the scissile bond and comes closest to mimicking the binding of good peptide substrates (Meyer et al., 1988b). The interaction pattern of this complex is similar to that observed in the HLE–TOM complex (Figures 2 and 5). The 24 backbone atoms superimpose with a rms deviation of 1.2 Å. As may be expected, the greatest variations are at the P_2 Pro and the terminal regions. Even though the residues fill the space quite well, the P_2'–P_3' Tyr-Thr terminus is relatively free to move within the van der Waals' surface of PPE's S′ binding region.

Primary Specificity Site (S_1). One-third of the total contacts between HLE and TOM are made by the P_1 residue (Leu-18I) of TOM (Figure 6). This pocket has its entrance between the flat sides of the peptide backbones of 214–216 and 191–192 and is constricted toward its bottom by residues Val-190, Phe-192, Ala-213, Val-216, and Phe-228 and the disulfide bridge Cys-191–Cys-220. The S_1 pocket has a hemispheric shape and is rather hydrophobic in character. Thus it is well adapted to accommodate medium-sized aliphatic side chains such as leucine and isoleucine. There is no specific anchoring point in the S_1 pocket, such as Asp-189 in trypsin, so that the aliphatic P_1 side chain is not fixed in a distinct orientation and can revolve like a ball and socket joint. Accommodation of larger side chains such as Phe would require a considerable expansion of the pocket, and as a consequence, substrates with P_1 phenylalanine are not normally cleaved by HLE.

In the structure of the valyl chloromethyl ketone–HLE complex (Wei et al., 1988), the β-branched bulky side chain of the P_1 valyl residue is accommodated with a slight tilting of its main chain. Simultaneously, the HLE S_1 pocket shrinks slightly and adapts to the reduced size of the smaller side chain. Serine proteases are generally characterized by the rigid "lock and key" model since no significant changes in conformation have been observed crystallographically upon binding of substrates or inhibitors. In the case of HLE, the lock and key model may have to be modified due to the small induced fit conformational changes observed upon binding of the chloromethyl ketone.

Leucine is slightly preferred over valine at P_1 among ovomucoid inhibitors (M. Laskowski, personal communication), in contrast to BPTI-derived HLE inhibitors, where valine seems to have the greater affinity (Tschesche et al., 1987). With nitroanilide substrates, a P_1 Val is favored over Leu (Zimmerman & Ashe, 1977); in the case of thiobenzyl ester substrates, the straight-chain Ape (Nva) has the highest k_{cat}/K_M value (relative values: Ape, 12.5; Ile, 5.3; Val, 4.1; Leu, 3.0; Ahe or Nle, 2.5; Met, 1.2; Ala, 1.0; Phe, 0; Harper

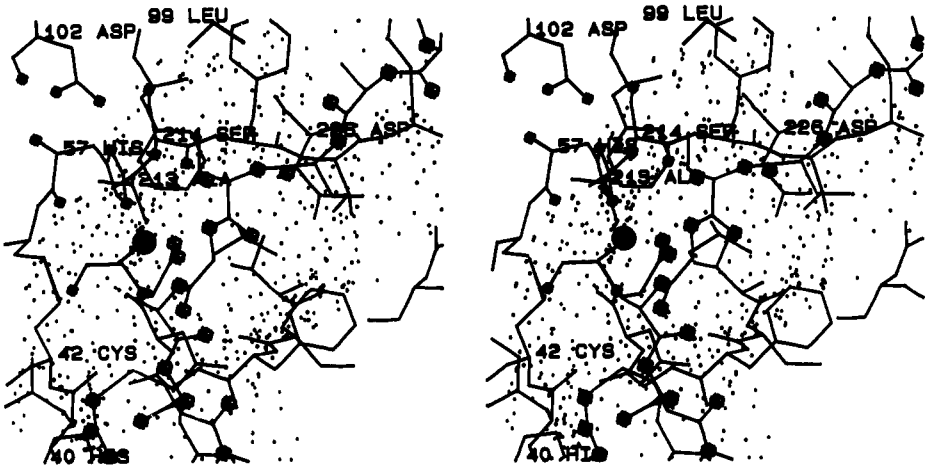

FIGURE 6: "Inside-out" view of the primary substrate specificity site (S_1) of HLE, as observed in the HLE–TOM complex. The heteroatoms of the inhibitor are represented by large spheres, and the catalytic tetrad of HLE is represented by small spheres. The double van der Waals' contact surface is represented as heavy dots. Superimposed on this is the contact surface of the PPE complex with the hexapeptide Thr-Pro-Ape-MeLeu-Tyr-Thr (small dots). This view depicts the marginally deeper S_1 pocket of HLE. Ser-195 Oγ is drawn as an enlarged sphere.

et al., 1984). Modeling predicts that an isoleucine side chain at P_1, with its Cδ atom trans to Cα, would fill the pocket of HLE even better than Leu, which is in accord with the solution experiments.

The P_1 residue of HLE's natural plasma inhibitor (α_1-protease inhibitor) is Met-358. Modeling experiments show that a methionine residue at P_1 should easily fit (with a typical bent conformation) into the S_1 pocket. Peptides with P_1 Met residues are reasonable HLE substrates, while oxidation of the Met to the sulfoxide results in decreased binding and absence of hydrolysis characterized by a significant drop in k_{cat}/K_M values (McRae et al., 1980; Nakajima et al., 1979). The extra oxygen of the methionine sulfoxide creates severe steric hindrance with the S_1 pocket, providing a structural basis for loss of the inhibitory capacity of α_1-protease inhibitor upon oxidation of Met-358 by cigarette smoke (Janoff et al., 1983; Matheson et al., 1982).

The bottom of the S_1 pocket in HLE contains an acidic residue, Asp-226, which is completely buried in the interior of the HLE molecule without any balancing counterion. The carboxylate group of Asp-226 is hydrogen-bonded with three interior water molecules which might serve to dissipate its negative charge. Asp-226 is somewhat shielded from the exterior of the pocket by Val-216 and Val-190. Model building experiments indicate that the gap between the side chains of Val-190 and Val-216 is just barely large enough to allow penetration of a basic side chain of a P_1 residue to form a salt link with Asp-226. Recent experiments have shown that HLE does not cleave either Lys or *S*-aminocysteine (an analogue of homolysine) substrates at significant rates, indicating that these substrates do not bind well in S_1 (T. Ueda and J. C. Powers, unpublished results).

The primary specificity pocket of PPE is slightly less hydrophobic and only marginally smaller in spite of considerable changes in the lining amino acids (Figures 3 and 6). This is consistent with PPE's perference for Ala and Nva (norvaline) rather than larger or branched amino acids in P_1 (Zimmerman & Ashe, 1977; Harper et al., 1984). In both elastases, residue 189 (Gly in HLE, Ser in PPE, Asp in trypsin) is not directly accessible to P_1 side chains. The bottom of the S_1 pocket in PPE is coated by the hydrophobic portion of Thr-226 (equivalent to Val-190 in HLE) and Ile-138 (Ser-138 of HLE is not accessible). The polar amino acid Gln-192 (Phe-192 in HLE) is located at the entrance to the pocket. Only Val-216 at the entrance, Phe-228, forming the "ceiling", and the disulfide bridge Cys-191–Cys-220 are common to both elastases (Figure 3).

Remaining Subsites. The second most important set of interactions in the HLE–TOM complex involves Thr-17I (P_2, Figure 2). The complementary subsite S_2, lined by Phe-215, Leu-99, and the flat side of the imidazole ring of His-57, is bowl-shaped and quite hydrophobic, but similar to that found in all other mammalian proteases, including PPE. Medium-sized hydrophobic side chains including proline are preferred.

The P_3 Cys-16I group is only in contact with HLE through main-chain atoms. More elongated side chains would, however, interact with hydrophobic surfaces of HLE, mainly with Phe-192 and Val-216. In common with interactions seen in other serine protease complexes with peptides, the P_3–S_3 contact is characterized by two intermolecular hydrogen bonds made with the backbone NH and carbonyl of Val-216. The side-chain Ala-15I (P_4) points along the side chains of residues Phe-215 and Arg-217 in HLE toward the bulk water. Interestingly, substrates with Lys at P_3 or P_4 are much less reactive than the corresponding Ala substrates (Yasutake & Powers, 1981). In contrast, the corresponding substrates with aromatic groups or large hydrophobic groups with a charge are more reactive than the corresponding Ala substrates. These substrates resemble desmosine, the charged hydrophobic cross-linking amino acid residue of elastin, and suggest that HLE may selectively bind to and cleave elastin near cross-linking regions through interaction at the S_3 and S_4 subsites.

The position and conformation of Pro-14I (P_5) are clearly dictated by intramolecular constraints in the ovomucoid inhibitor itself. The very weak hydrogen bond formed between the NH of Gly-218 in HLE with the carbonyl of P_5 may not be representative of binding of substrates with flexible peptide chains. Addition of a P_5 residue in most cases increases the reactivity of substrates (Wenzel & Tschesche, 1981; Lestienne & Bieth, 1980).

On the leaving group side of the scissile bond, Tyr-20I (P_2') of TOM makes by far the most contacts with HLE, mainly with Ile-151. Affinity measurements with ovomucoid variants lacking tyrosine emphasize the favorable interaction made by the phenolic side chain at this subsite (M. Laskowski, personal communication). Arg-21I (P_3') nestles with its (primary hydrophobic) side chain and the flat side of its guanidino group toward the quite hydrophobic surface of HLE's S_3' subsite. This shallow subsite is formed mainly by the side chains of Phe-41, Leu-35, and Val-63 and probably represents the hy-

drophobic subsite that binds peptide inhibitors [e.g., Boc-Val-Val-Val-NH$(CH_2)_{11}CH_3$, K_I = 0.21 μM] with long carboxyl-terminal aliphatic chains (Lentini et al., 1987).

The S_1' subsite consists of a relatively hydrophobic pocket lined by Cys-42–Cys-58 and Phe-41 and can accommodate all amino acid residues at P_1', with the exception of Pro, other N-methylated residues, and large hydrophobic residues (e.g., Trp). In the ovomucoid inhibitors, Glu-19I (P_1') forms an intramolecular hydrogen bond with Thr-17I (P_2). This hydrogen bond becomes stronger in the course of complex formation and makes a significant contribution to the overall binding of ovomucoid inhibitors to serine proteases (M. Laskowski, personal communication). Thus, a cyclic structure containing this tripeptide segment (P_2–P_1') might be an excellent template for the design of potent new HLE inhibitors.

In general, the PPE subsites are less hydrophobic than those in HLE (Figure 3). This is most apparent for subsites at extreme ends of the substrate binding site (S_5–S_6 and S_3'), but is also true for sites in the immediate vicinity of the specificity pocket (Phe-192 and Phe-41 in HLE compared to Gln-192 and Thr-41 in PPE). The substantial increase in hydrophobic character and the reduced capability to form hydrogen bonds may explain the unique property of HLE to be inhibited by cis-unsaturated oleic acids and other related fatty acids (Ashe & Zimmerman, 1977). In addition, many hydrophobic peptide and heterocyclic inhibitors are much more reactive with HLE than PPE.

Specificity and Mechanism

Interactions at remote subsites can profoundly influence the catalytic mechanism and specificity of both elastases. With nitroanilide substrates of HLE, extension of the peptide chain by the addition of a P_3 residue results in an 100-fold increase in the acylation rate and a change in the rate-limiting step from acylation to deacylation (Stein et al., 1987a). There also appears to be communication between remote subsites and the S_1 pocket because some amino acid residues (e.g., Phe) are tolerated in monomeric reactive substrates and not in extended substrates (Stein, 1985). In addition, proton inventory studies have shown that minimal substrates (monomeric or dipeptides) are hydrolyzed by simple general-base catalysis by His-57 involving transfer of one proton in the rate-limiting transition state (Stein et al., 1987b). However, tri- and tetrapeptides are hydrolyzed by a mechanism that involves full functioning of the catalytic triad and transfer of two protons in the rate-limiting step.

The P_3–S_3 contact (Figure 3) is characterized by the two intermolecular hydrogen bonds made with the backbone NH and carbonyl of Val-216. Clearly this interaction communicates directly with the S_1 subsite since the isopropyl side chain of Val-216 forms one side of the pocket and the pocket changes slightly in size upon binding the tetrapeptide valyl chloromethyl ketone inhibitor. Communication with the catalytic triad may involve the hydrogen-bonding network between Asp-102 and Ser-214, which in turn is part of the peptide backbone (including Val-216) that forms the β-sheet structure with a peptide substrate. Indeed, Ser-214 is conserved in serine proteases and forms a catalytic tetrad with Ser-195, His-57, and Asp-102.

Peptide inhibitors such as TOM possess a reactive-site sequence that matches that of an ideal substrate and yet is cleaved extremely slowly. Nature has devised a number of "tricks" to keep this bond intact: complementary surfaces of enzyme binding sites and inhibitor binding segments; restricted mobility of binding loops within the enzyme–inhibitor complex; and favorable hydrogen bonds. The rate of cleavage of the hexapeptide Thr-Pro-Ape*MeLeu-Tyr-Thr might be slowed down because stereochemical inversion at the P_1' nitrogen atom of the scissile peptide bond in N-methylated P_1' substrates is internally restricted (Bizzozero & Zweifel, 1975; Bizzozero & Dutler, 1981) due to stereoelectronic control (Deslongchamps, 1975). A similar rationale could be used to explain the stability of complexes of proteases with TOM and other protein protease inhibitors.

Synthetic Elastase Inhibitors

Peptide Chloromethyl Ketone and Fluoro Ketone Inhibitors. Peptide halo ketone inhibitors have been widely investigated with serine proteases, and several crystal structures of serine proteases complexed with peptide chloromethyl ketones have been reported previously [see Powers (1977) and Powers and Harper (1986) for reviews]. The existence of the extended substrate binding site composed of the backbone atoms of 214–216 was first demonstrated in chloromethyl ketone serine protease structures. With chloromethyl ketones, two bonds are formed between the enzyme and inhibitor: one between His-57 and the methylene group of the inhibitor and one between the Ser-195 and the ketonic carbonyl group. In the HLE complex with MeO-Suc-Ala-Ala-Pro-Val-CH_2Cl (Figure 4), similar covalent bonds are formed between the methylene group of the P_1 valine chloromethyl ketone residue and Nϵ of His-57 of HLE and between the Val carbonyl group and Oγ of Ser-195. The P_1 residue is pulled toward the S_1 pocket, with a simultaneous strengthening of the hydrogen bond between the P_1 amide nitrogen and the amide carbonyl of Ser-214 (Figure 3) and with pyramidalization of its carbonyl group with the addition of Oγ of Ser-195. This structure is similar to the presumed tetrahedral intermediate formed during serine protease peptide bond cleavage.

Peptide fluoro ketones are potent reversible inhibitors of HLE, PPE, and other serine proteases (Stein et al., 1987c; Imperali & Abeles, 1986; Trainor, 1987). These inhibitors, unlike chloromethyl ketones, are not potent alkylating agents and have greater therapeutic potential. The structures of two fluoro ketones bound to PPE have been determined (Figure 4; Takahashi et al., 1988b, 1989). Both form tetrahedral adducts with Ser-195 of PPE. In both the Ac-Ala-Pro-Val-CF_3 complex (K_I = 9.5 μM, pH 5.5) and the Ac-Ala-Pro-Val-CF_2CO-NH-$CH_2CH_2C_6H_5$ complex (K_I = 5.5 μM, pH 5.5), the oxyanion oxygen atom (derived from the fluoroketone carbonyl) is located in the oxyanion hole and forms hydrogen bonds with the NH of Ser-195 and Gly-193. The imidazole ring of His-57, occupying the "in" position also observed in native PPE, forms hydrogen bonds with a water molecule and with one fluorine atom of each inhibitor. The two inhibitors form antiparallel β-sheet structures with residues 214–216 of PPE. Comparison of the peptide backbone of the trifluoromethyl ketone bound to PPE with the HLE–chloromethyl ketone complex gives an excellent rms agreement of 0.38 Å when the 12 common backbone atoms are superimposed.

Heterocyclic Inhibitors. A wide variety of heterocyclic compounds have been described as inhibitors for serine proteases, including β-lactams, isocoumarins, benzoxazinones, pyrones, and saccharin derivatives (Powers & Harper, 1986). Such heterocyclic compounds are much more likely to yield practical therapeutic agents than peptide inhibitors, which are often poorly adsorbed and are often cleaved by other proteases. The crystal structures of four heterocyclic complexes have been determined to high resolution with PPE: the isostructural benzoxazinones (Radhakrishnan et al., 1987) and two isocoumarins (Meyer et al., 1985; R. Radhakrishnan and E. F. Meyer, unpublished results).

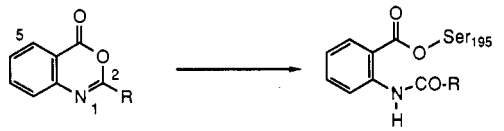

FIGURE 7: Mechanism of inhibition of elastase by benzoxazinone inhibitors.

Substituted benzoxazin-4-ones are potent inhibitors of HLE and PPE along with other serine proteases (Teshima et al., 1982). Benzoxazin-4-ones with 2-alkyl or fluoroalkyl substituents are particularly potent with K_I values as low as 92 nM, probably due to an interaction of the alkyl substituent with the S_1 pocket. The mechanism of benzoxazinone inhibition involves reaction with Ser-195 to form stable acyl enzyme derivatives (Stein et al., 1987d; Figure 7). The acylation rates, deacylation rates, and hydrolytic stability of the benzoxazin-4-ones can be altered by changing the nature of the substituents in both rings (Spencer et al., 1986; Krantz et al., 1987). Electron-withdrawing substituents on both rings increase the acylation and hydrolysis rates, electron-donating substituents increase stability, and bulky substitutes often slow the deacylation rates.

Two isomorphous benzoxazinone complexes, 5-Me-2-[Boc-NHCH(*i*-Pr)]benzoxazin-4-one and 5-Cl-2-[Boc-NHCH(*i*-Pr)]benzoxazin-4-one, have been studied crystallographically (Table II; Radhakrishnan et al., 1987). The resultant, isomorphous structures have an 8-Cl or 8-Me group pointing into the S_1 primary specificity site. The hydrophobic Boc-Val groups make van der Waals contacts with both the S_2' or S_1' sites of the enzymic receptor site (Figure 11).

In all PPE complexes with heterocyclic inhibitors thus far studied, the imidazole ring of His-57 is observed in the "out" position; in the place of the "in"-positioned imidazole ring, a water molecule is always found bridging the Asp-102 carboxylate with the benzoyl carbonyl group of the heterocycle or with Ser-195 Oγ. Surprisingly, the benzoyl ester group formed upon reaction with Ser-195 is not in the oxyanion hole but is rather directed to the new water molecule. Instead, the valyl carbonyl group, newly formed during the opening of the benzoxazinone ring, is located in the oxyanion hole. Thus deacylation seems in this case not to be facilitated by oxyanion hole activation, and this may be the reason for the slow hydrolysis of this complex. It is likely that the bulky Boc and *i*-Pr groups of the inhibitor, by leverage through the phenyl group of the opened benzoxazinone ring, contribute to this particular conformation. Benzoxazinone inhibitors without bulky groups might thus be bound in quite different conformations in the active site of PPE.

Isocoumarin Inhibitors. Isocoumarins are one class of heterocyclic structures that are rich in possible masked functional groups. Thus far, isocoumarins containing latent acid chloride (or ketenes) and quinone imine methide functional groups have been described as serine protease inhibitors. The initial reaction involves an acylation of Ser-195 of the serine protease by the isocoumarin ring carbonyl to form an acyl enzyme in which the isocoumarin ring is opened and new functional groups are unmasked. These acyl enzymes are often quite stable, but with the appropriately substituted isocoumarins, further reactions can occur between the newly released reactive groups and the side chains of neighboring amino acid residues of the enzyme.

HLE and PPE are both inhibited effectively by 3,4-dichloroisocoumarin with $k_{obsd}/[I]$ values of 8900 and 2500 M^{-1} s^{-1}, respectively (Harper et al., 1985). Although the elastases are most effectively inhibited, dichloroisocoumarin is a more

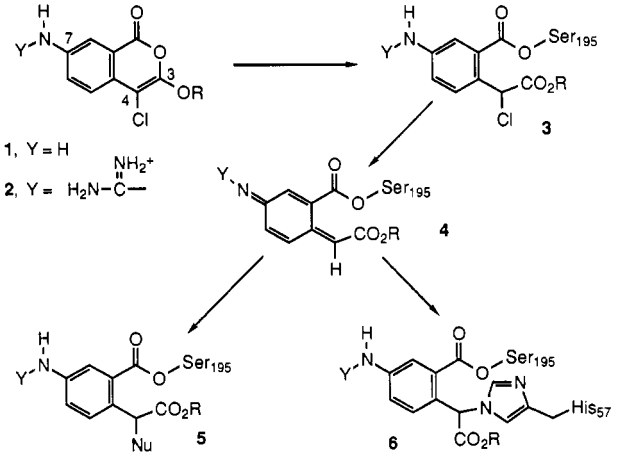

FIGURE 8: Mechanism of inhibition of elastase by isocoumarin inhibitors.

general serine protease inhibitor and reacts with all serine proteases that have been observed thus far. Increased specificity and reactivity have been observed with 3-alkoxy-7-amino-4-chloroisocoumarins (Figure 8, **1**) containing varous substituents on the 7-amino group and in the 3-position (Harper & Powers, 1985). In the initial enzyme–inhibitor complex, the 3-alkoxy group is probably interacting with the S_1 pocket because derivatives with small alkoxy groups (3-methoxy, 3-ethoxy, 3-propoxy) inhibit HLE and PPE most effectively, while those with aromatic groups (3-benzyloxy) inhibit chymotrypsin and rat mast cell protease II most effectively.

The available evidence points to the inactivation mechanism shown in Figure 8. Enzyme acylation results in the formation of an acyl enzyme (**3**), which can undergo an elimination reaction to produce a 4-quinone imine methide (**4**) in the active site. This can react either with an enzyme nucleophile (probably His-57) to give an irreversibly inhibited enzyme structure (**6**) or with a solvent nucleophile to give a stable acyl enzyme (**5**). Partial reactivation by hydroxylamine (42% at pH 7.5 with PPE) suggests a partitioning between the two enzyme–inhibitor complexes in solution with the residual 58% probably representing the nonreactivatable complex **6** containing an alkylated histidine residue. Both the 7-amino and 4-chloro groups are required for formation of a stable inactivated enzyme; isocoumarins that lack these features inhibit serine proteases but deacylate fairly rapidly.

The crystal structures of two complexes of isocoumarins with PPE have been solved to atomic resolution (Table II). The structure analysis of PPE inactivated by 7-amino-4-chloro-3-methoxyisocoumarin at pH 5 in 0.1 M acetate buffer (Meyer et al., 1985) confirmed the postulated acylation mechanism concurrent with isocoumarin ring–ester cleavage since a single ester bond was formed with Ser-195 of PPE. It also contained an element of surprise: an acetate ion from the buffer had displaced the chlorine stereospecifically to give a stable acyl enzyme (Figure 8, **5**, Nu = acetoxy). The resulting structure has the acetoxy group in the S_1 pocket, the methoxy of the ester extends out into solution, and the benzoyl carbonyl points approximately into the oxyanion hole. The carbonyl group of the carbomethoxy moiety forms a hydrogen bond with His-57. The 7-amino group points toward the bulk water and makes no important intermolecular contacts.

Isocoumarins with basic substitutes such as 3-alkoxy-4-chloro-7-guanidinoisocoumarin (**2**) are potent inhibitors for trypsin, blood coagulation enzymes (Kam et al., 1988), complement enzymes, and natural killer cell tryptases (Hudig et

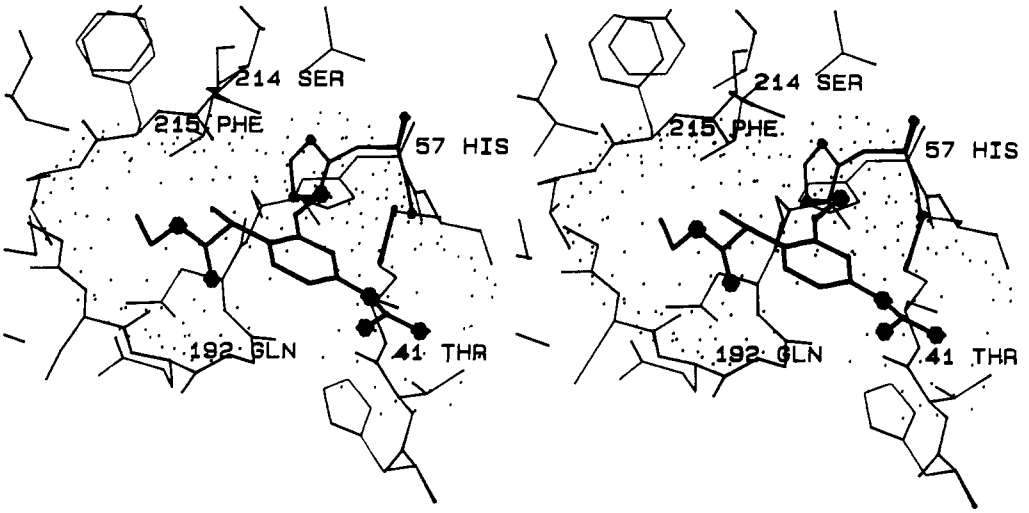

FIGURE 9: Stereo drawing of the complex formed upon reaction of PPE with 4-chloro-3-ethoxy-7-guanidinoisocoumarin. The heteroatoms of the inhibitor are drawn as spheres. His-57 in native PPE is drawn with heavier lines in the "in" orientation, as found in the native enzyme and peptide complexes. In this complex, the imidazole ring of His-57 (thin lines) is shifted to the "out" position, stacking on the phenyl group of the inhibitor. The ethoxy group of the inhibitor is in the S_1 pocket (center left), and the guanidino group is hydrogen-bonded to Thr-41. The covalent bond between the inhibitor and Ser-195 Oγ has not been drawn. The interface contact surface is depicted as small dots.

al., 1987). Unexpectedly, 4-chloro-3-ethoxy-7-guanidinoisocoumarin (**2**, R = Et) proved to be a potent inhibitor of HLE ($k_{obsd}/[I]$ = 81 000 M^{-1} s^{-1}) and a slow inhibitor of PPE ($k_{obsd}/[I]$ = 2300 M^{-1} s^{-1}). Due to its good solubility, it reacted readily with crystals of PPE (Figure 9; E. F. Meyer and R. Radhakrishnan, unpublished results). As in the cases of the other benzoxazinone and isocoumarin inhibitors, the reaction product is covalently bound to Ser-195 Oγ (Figure 9). The ethoxy group is found in the S_1 pocket, in agreement with the P_1 preference of PPE for small hydrophobic groups.

The phenyl group is approximately parallel to and in van der Waals contact with the outward rotated imidazole groups of His-57. The chlorine atom of the isocoumarin has not been displaced but is near His-57. The 7-guanidino group makes three good hydrogen bonds to Thr-41. The benzoyl carbonyl group produced by the isocoumarin ring opening is not located in the oxyanion hole, perhaps again explaining the stability of the complex toward deacylation. The enzyme contains no charge-compensating groups near the 7-guanidino moiety.

Molecular modeling of the 7-guanidinoisocoumarin–PPE complex suggested that the addition of small alkyl groups (*tert*-butyl) to the guanidino group might increase affinity due to the presence of a small hydrophobic pocket near the terminal nitrogen atom of the guanidino group. Indeed, replacement of the 7-H_2N–C(=NH_2^+)–NH group with a *tert*-butyl–NH–CO–NH– group led to a 3.5-fold increase in $k_{obsd}/[I]$ (both the 7-guanidino and the 7-H_2N–CO–NH variants are equally potent inhibitors, and the *tert*-butylurea derivative was synthetically more accessible than a *tert*-butylguanidine derivative).

Thr-41 is replaced in HLE by Phe-41, which cannot form the same side-chain hydrogen bonds with the guanidino group. Thus it is not clear why 4-chloro-3-ethoxy-7-guanidinoisocoumarin is such a good inhibitor of HLE and whether it indeed binds in the same manner as with PPE. However, replacement of the 7-guanidino group with large aromatic acyl groups such as 7-(Tos-Phe-NH-) yields even more potent HLE inhibitors ($k_{obsd}/[I]$ = 190 000 M^{-1} s^{-1}; Harper & Power, 1985), which could partially be explained by an interaction with Phe-41 in HLE.

β-Lactam Elastase Inhibitors. β-Lactam antibiotics are widely prescribed and well-tolerated inhibitors of D-Ala-D-Ala transpeptidases and other enzymes involved in bacterial cell wall biosynthesis. The active drugs typically have a free carboxyl group and are thought to mimic D-Ala-D-Ala. Medicinal chemists have tailored other β-lactams to inhibit some β-lactamases. A group at Merck recognized the similarity of these β-lactamases to serine proteases and tested β-lactams as inhibitors of HLE. Esters of cephalosporin and other β-lactams were thus discovered to be potent acylating inhibitors of HLE (Doherty et al., 1986). In contrast to other enzymes inhibited by β-lactams, HLE requires the carboxyl group of the antibiotic to be esterified for effective inhibition. The cephalosporin *tert*-butyl ester shown in Figure 10 irreversibly inhibits HLE (K_I = 0.18 μM; k_2/K_I = 161 000 M^{-1} s^{-1}). Most of the derivatives reported were also excellent inhibitors of PPE.

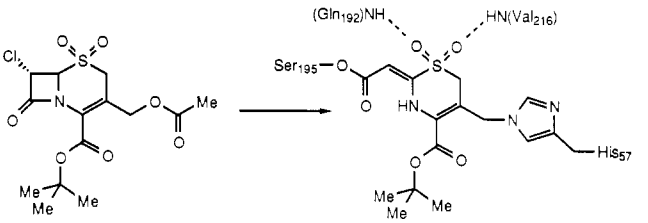

FIGURE 10: Structure of the acyl enzyme formed upon inhibition of PPE by a cephalosporin β-lactam inhibitor.

The structure of PPE inhibited by 3-(acetoxymethyl)-7α-chloro-3-cephem-4-carboxylate 1,1-dioxide (Figure 10) has been determined (Navia et al., 1987). Two bonds are formed between the inhibitor and the enzyme, an ester linkage with Ser-195 and a bond between the imidazole ring of His-57 and the 3′-methylene group. During the inhibition reaction, the β-lactam ring is opened and both the chloro and acetoxy groups are lost, obviously an excellent example of a mechanism-based or suicide inhibitor. In addition to the two covalent bonds, the sulfone oxygen atoms are hydrogen-bonded to the NH of Val-216 and the side chain of Gln-192. The 7′α-chloro group probably occupies the S_1 pocket during the initial acylation reaction, while the *tert*-butyl group fits at the edge of a large open area on the periphery of the enzyme.

Modeling and Inhibitor Design

Due to the absence of strong (i.e., Coulombic) interactions in elastase–ligand complexes, these studies have helped to

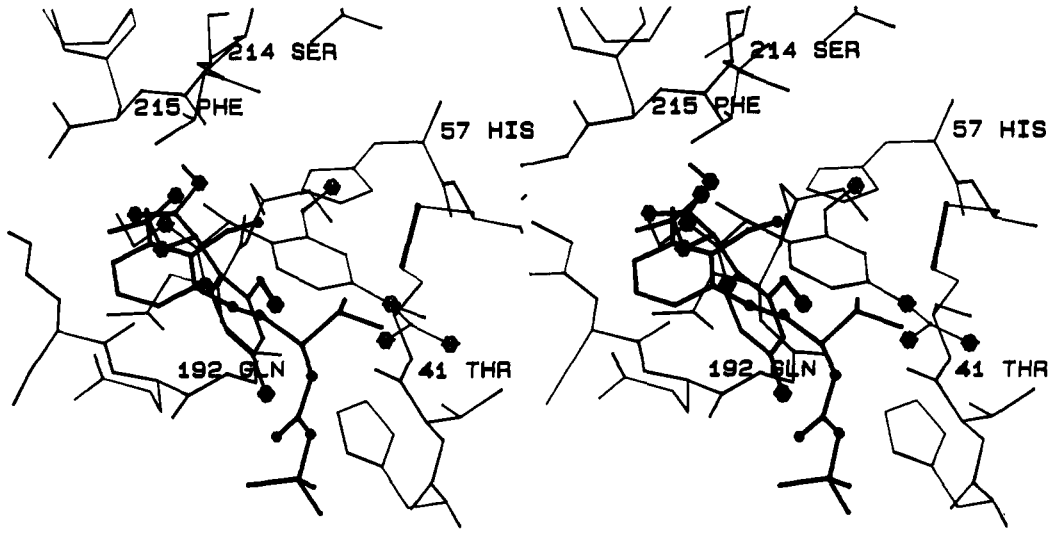

FIGURE 11: Stereo drawing of the strikingly different orientations of three heterocyclic inhibitors bound to the active site of PPE. The PPE complex with 5-Cl- or 5-Me-2-[Boc-NHCH(*i*-Pr)]benzoxazinone is drawn with heavy lines. The *tert*-butyl group of the inhibitor reaches down to the S_2' subsite of PPE, and the 5-chloro (or 5-methyl) substituent of the inhibitor is in the primary (S_1) specificity pocket (center left). Lines of intermediate thickness depict the 7-amino-4-chloro-3-methoxyisocoumarin complex. An acetate has displaced chloride from the inhibitor and occupies the S_1 pocket. The benzoyl carbonyl oxygen atom is in the oxyanion hole. Thin lines are used to depict the 4-chloro-3-ethoxy-7-guanidinoisocoumarin complex with PPE in the same orientation as in Figure 8. The PPE active-site conformation depicted here corresponds to the recently determined structure of the complex of PPE with 4-chloro-3-ethoxy-7-guanidinoisocoumarin (Figure 8).

define the decisive role played by weak (i.e., van der Waals) interactions in enzyme–ligand interactions. A common factor of the elastase–inhibitor complexes is the close fit of van der Waals interaction surfaces between the inhibitor structure and the convoluted surface of the enzyme. A remarkable feature of the PPE complexes formed with heterocyclic inhibitors is the variety of binding modes of chemically and structurally related compounds (Figure 11). This observation must be regarded as a "caveat" to chemists who wish to use an analogous crystal structure for molecular modeling and inhibitor design. We clearly do not yet know all the rules for predicting a preferred binding conformation of a small molecule inhibitor to the active site of these enzymes. Energy minimization is an obedient servant which will bring a proposed model structure to its local minimum, but molecular dynamics and energy minimization methods still must be improved considerably to generate the actual conformation. Thus, there is a compelling need for additional structural information on many complexes of small molecule inhibitors of varying structures with elastases and other serine proteases. Only with such information in hand will it be possible to model new inhibitor structures into the active sites of serine proteases with any degree of confidence.

Summary and Future Directions

The crystal structures of HLE and PPE with peptides and peptide derivatives are remarkably similar (a property shared with other homologous serine proteases). Both enzymes have similar primary substrate specificities by virtue of the similar geometric and hydrophobic character of their S_1 binding pockets. However, the enhanced hydrophobicity of the HLE active site compared with the PPE active site that corresponds to differences in primary sequence is probably responsible for its affinity for longer aliphatic chains at the P_1 residue of substrates and for the binding of long alkyl chain inhibitors (e.g., oleic acid).

In contrast to peptide derivatives, the crystal structures of heterocyclic inhibitors of PPE show dramatic differences. Again the increased reactivity of hydrophobic inhibitors, such as isocoumarins for HLE, may reflect the increased hydrophobicity of the HLE active site. Molecular modeling of the crystal structures, when used with caution, often provides new insights into the binding mode of inhibitors, suggests ways to exploit differences in homologous enzymes to improve specificity, and leads to the discovery of novel inhibitor structures.

A variety of elastase inhibitors have been shown to be effective in animal models of pulmonary emphysema, inflammation, and other related diseases (Powers & Bengali, 1986). These include peptide chloromethyl ketones (Stone et al., 1981), peptide aldehydes (Hassal et al., 1985), peptide boronic acids (Sosket et al., 1986), β-lactams (Doherty et al., 1986), and the protein protease inhibitor eglin c. Human α_1-protease inhibitor has already been used in therapy with PiZ (α_1-protease inhibitor deficiency) patients (Gadek et al., 1981). Several additional inhibitors will be tested in the near future for treatment of disease in humans. At present it is most likely that practical therapeutic drugs will originate from either the β-lactam, peptide boronic acid, or peptide fluoro ketone classes of elastase inhibitors since current classes of heterocyclic inhibitors suffer from low plasma stability. The structural information obtained with elastase–inhibitor complexes should be invaluable for future design work with all classes of elastase inhibitors and should improve the prospects for the treatment of chronic diseases such as pulmonary emphysema.

Acknowledgments

We thank Dr. James Travis and his research group at the University of Georgia for the neutrophil enzymes used in this research and for many hours of valuable and stimulating discussions.

References

Aoki, Y. (1978) *J. Biol. Chem. 253*, 2026–2032.
Ashe, B. M., & Zimmerman, M. (1977) *Biochem. Biophys. Res. Commun. 75*, 184–189.
Baici, A., & Seemueller, U. (1984) *Biochem. J. 218*, 829–833.
Baici, A., Salgam, P., Fehr, K., & Boni, A. (1980) *Biochem. Pharmacol. 29*, 1723–1727.
Baugh, R. J., & Travis, J. (1976) *Biochemistry 15*, 836–841.

Bieth, J. G. (1986) in *Regulation of Matrix Accumulation* (Mechan, R. D., Ed.) pp 217–320, Academic Press, New York.

Birktoft, J. J., & Blow, D. M. (1972) *J. Mol. Biol. 68*, 187–240.

Bizzozero, S. A., & Zweifel, B. O. (1975) *FEBS Lett. 59*, 105–108.

Bizzozero, S. A., & Dutler, H. (1981) *Bioorg. Chem. 10*, 46–62.

Bode, W., & Schwager, P. (1975) *J. Mol. Biol. 98*, 693–717.

Bode, W., & Huber, R. (1986) in *Molecular and Cellular Basis of Digestion* (Desnuelle, P., Sjostrom, H., & Noren, O., Eds.) pp 213–234, Elsevier, Amsterdam.

Bode, W., Chen, Z., Bartels, K., Kutzbach, C., Schmidt-Kastner, G., & Bartunik, H. (1983) *J. Mol. Biol. 164*, 237–282.

Bode, W., Papmokos, E., Musil, D., Seemueller, U., & Fritz, H. (1986a) *EMBO J. 5*, 813–818.

Bode, W., Wei, A.-Z., Huber, R., Meyer, E., Travis, J., & Neumann, S. (1986b) *EMBO J. 5*, 2453–2458.

Braun, N. J., Bodmer, J. L., Virca, G. D., Metz-Virca, G., Maschler, R., Bieth, J. G., & Schnebli, H.-P. (1987) *Biol. Chem. Hoppe-Seyler 368*, 299–308.

Clore, G. M., Gronenborn, A. M., Carlson, G., & Meyer, E. (1986) *J. Mol. Biol. 190*, 259–267.

Cohen, G. H., Silverton, E. W., & Davies, D. (1981) *J. Mol. Biol. 148*, 449–479.

Deslongchamps, P. (1977) *Heterocycles 7*, 2463–2490.

Doherty, J. B., Ashe, B. M., Argenbright, L. W., Barker, P. L., Bonney, R. J., Chandler, G. O., Dahlgren, M. E., Dorn, C. P., Finke, P. E., Firestone, R. A., Fletcher, D., Hagmann, W. K., Mumford, R., O'Grady, L., Maycock, A. L., Pisano, J. M., Shah, S. K., Thompson, K. R., & Zimmerman, M. (1986) *Nature 322*, 192–194.

Farley, D., Salvesen, G., & Travis, J. (1988) *Biol. Chem. Hoppe-Seyler 369 (Suppl.)*, 3–7.

Fujinaga, M., & James, M. N. G. (1987) *J. Mol. Biol. 195*, 373–396.

Gadek, J. E., Klein, H. G., Holland, P. V., & Crystal, R. G. (1981) *J. Clin. Invest. 68*, 1158–1165.

Gruetter, M. G., Fendrich, G., Huber, R., & Bode, W. (1988) *EMBO J. 7*, 345–351.

Harper, J. W., & Powers, J. C. (1985) *Biochemistry 24*, 7200–7213.

Harper, J. W., Cook, R. R., Roberts, C. J., McLaughlin, B. J., & Powers, J. C. (1984) *Biochemistry 23*, 2995–3002.

Harper, J. W., Hemmi, K., & Powers, J. C. (1985) *Biochemistry 24*, 1831–1841.

Hartley, B. S. (1964) *Nature 201*, 1284.

Hassall, C. H., Johnson, W. H., & Roberts, N. A. (1979) *Bioorg. Chem. 8*, 299–309.

Hassal, C. H., Johnson, W. H., Kennedy, A. J., & Roberts, N. A. (1985) *FEBS Lett. 183*, 201–205.

Huber, R., & Bode, W. (1978) *Acc. Chem. Res. 11*, 114–122.

Hudig, D., Gregg, N. J., Kam, C., & Powers, J. C. (1987) *Biochem. Biophys. Res. Commun. 149*, 882–888.

Hughes, D. L., Sieker, L. C., Bieth, J., & Dimicoli, J. L. (1982) *J. Mol. Biol. 162*, 645–658.

Imperiali, B., & Abeles, R. (1986) *Biochemistry 25*, 3760–3767.

Janoff, A., Carp, H., Laurent, P., & Raju, L. (1983) *Am. Rev. Respir. Dis. 127*, 31–38.

Kam, C., Fujikawa, K., & Powers, J. C. (1988) *Biochemistry 27*, 2547–2557.

Krantz, A., Spencer, R. W., Tam, T. F., Thomas, E., & Copp, L. J. (1987) *J. Med. Chem. 30*, 589–591.

Kraut, J. (1977) *Annu. Rev. Biochem. 46*, 331–358.

Laskowski, M., & Kato, I. (1980) *Annu. Rev. Biochem. 49*, 593–626.

Lentini, A., Farchione, F., Bernai, B., Kreula-Ongarjnukool, N., & Tovivich, P. (1987) *Biol. Chem. Hoppe-Seyler 368*, 369–378.

Lestienne, P., & Bieth, J. (1980) *J. Biol. Chem. 255*, 9289–9294.

MacDonald, R. J., Swift, G. H., Quinto, C., Swain, W., Pictet, R. L., Nikovits, W., & Rutter, W. J. (1982) *Biochemistry 21*, 1453–1463.

Marquart, M., Walter, J., Deisenhofer, J., Bode, W., & Huber, R. (1983) *Acta Crystallogr. B39*, 480–490.

Matheson, N. R., Janoff, A., & Travis, J. (1982) *Mol. Cell. Biochem. 45*, 65–71.

McRae, B., Nakajima, K., Travis, J., & Powers, J. C. (1980) *Biochemistry 19*, 3973–3978.

Meyer, E., Presta, L. G., & Radhakrishnan, R. (1985) *J. Am. Chem. Soc. 107*, 4091–4093.

Meyer, E. F., Radhakrishnan, R., Cole, G. M., & Presta, L. G. (1986) *J. Mol. Biol. 189*, 533–539.

Meyer, E. F., Cole, G., Radhakrishnan, R., & Epp, O. (1988a) *Acta Crystallogr. B44*, 26–38.

Meyer, E. F., Clore, G. M., Gronenborn, A. M., & Hansen, H. A. S. (1988b) *Biochemistry 27*, 725–730.

Nakajima, K., Powers, J. C., & Zimmerman, M. (1979) *J. Biol. Chem. 254*, 4027–4032.

Navia, M. A., Springer, J. P., Lin, T.-Y., Williams, H. R., Firestone, R. A., Pisano, J. M., Doherty, J. B., Finke, P. E., & Hoogsteen, K. (1987) *Nature 327*, 79–82.

Navia, M. A., McKeever, B. M., Springer, J. P., Lin, T.-Y., Williams, H. R., Fluder, E. M., Dorn, C. D., & Hoogsteen, K. (1989) *Proc. Natl. Acad. Sci. U.S.A. 86*, 7–11.

Neurath, H. (1986) *J. Cell. Biochem. 32*, 35–49.

Okano, K., Aoki, Y., Sakurai, T., Kajitani, M., Kanai, S., Shimazu, H., & Naruto, M. (1987) *J. Biochem. 102*, 13–16.

Papamokos, E., Weber, E., Bode, W., Huber, R., Empie, M. W., Kato, I., & Laskowski, M. (1982) *J. Mol. Biol. 158*, 515–537.

Powers, J. C. (1977) in *Chemistry and Biochemistry of Amino Acids, Peptides and Proteins* (Weinstein, B., Ed.) Vol. 4, pp 65–178, Marcel Dekker, New York.

Powers, J. C., & Bengali, Z. H. (1986) *Am. Rev. Respir. Dis. 134*, 1097–1100.

Powers, J. C., & Harper, J. W. (1986) in *Proteinase Inhibitors* (Barrett, A. J., & Salvensen, G., Eds.) pp 55–152, Elsevier, Amsterdam.

Powers, J. C., Gupton, B. F., Harley, A. D., Nishino, N., & Whitley, R. J. (1977) *Biochim. Biophys. Acta 485*, 156–166.

Radhakrishnan, R., Presta, L. G., Meyer, E. F., & Wildonger, R. (1987) *J. Mol. Biol. 198*, 417–424.

Remington, S. J., Woodbury, R. G., Reynolds, R. A., Matthews, B. W., & Neurath, H. (1988) *Biochemistry 27*, 8097–8105.

Rosenberg, S., Barr, P. S., Najarian, R., & Hallewell, R. A. (1984) *Nature 312*, 77–80.

Sawyer, L., Shotton, D. M., Campbell, J. W., Wendell, P. L., Muirhead, H., Watson, H. C., Diamond, R., & Ladner, R. C. (1978) *J. Mol. Biol. 118*, 137–208.

Schechter, I., & Berger, A. (1967) *Biochem. Biophys. Res. Commun. 27*, 157–162.

Seemueller, U., Arnhold, M., Fritz, H., Wiedenmann, K., Machleidt, W., Heinzel, R., Appelhans, H., Gassen, H. G.,

& Lottspeich, F. (1986) *FEBS Lett. 199*, 43–48.
Shen, W.-F., Fletcher, T. S., & Largman, C. (1987) *Biochemistry 26*, 3447–3452.
Shotton, D. M., & Hartley, B. S. (1970) *Nature 225*, 802–806.
Shotton, D. M., & Watson, H. C. (1970) *Nature 225*, 811–816.
Sinha, S., Watorek, W., Karr, S., Giles, J., Bode, W., & Travis, J. (1987) *Proc. Natl. Acad. Sci. U.S.A. 84*, 2228–2232.
Soskel, N. T., Watanabe, S., Hardie, R., Shenvi, A. B., Punt, J. A., & Kettner, C. (1986) *Am. Rev. Respir. Dis. 133*, 639–642.
Spencer, R. W., Copp, L. J., Bonaventura, B., Tam, T. F., Liak, T. J., Billedeau, R. J., & Kranz, A. (1986) *Biochem. Biophys. Res. Commun. 140*, 928–933.
Stein, R. L. (1985) *Arch. Biochem. Biophys. 236*, 677–680.
Stein, R. L., Strimpler, A. M., Hori, H., & Powers, J. C. (1987a) *Biochemistry 26*, 1301–1305.
Stein, R. L., Strimpler, A. M., Hori, H., & Powers, J. C. (1987b) *Biochemistry 26*, 1305–1314.
Stein, R. L., Strimpler, A. M., Edwards, P. E., Lewis, J. J., Mauger, R. C., Schwartz, J. A., Stein, M. M., Trainor, D. A., Wildonger, R. A., & Zottola, M. A. (1987c) *Biochemistry 26*, 2682–2689.
Stein, R. L., Strimpler, A. M., Viscarello, B. R., Wildonger, R. A., Mauger, R. C., & Trainor, D. A. (1987d) *Biochemistry 26*, 4126–4130.
Stone, P. J., Lucey, E. C., Calore, J. D., Snider, G. L., Franzblau, C., Castillo, M. J., & Powers, J. C. (1981) *Am. Rev. Respir. Dis. 124*, 56–59.
Takahashi, H., Nukiwa, T., Basset, T., & Crystal, R. G. (1988a) *J. Biol. Chem. 263*, 2543–2547.
Takahashi, L. H., Radhakrishnan, R., Rosenfield, R. E., Meyer, E. F., Trainor, D. A., & Stein, M. (1988b) *J. Mol. Biol. 201*, 423–428.
Takahashi, L. H., Radhakrishnan, R., Rosenfield, R. E., Meyer, E. F., & Trainor, D. A. (1989) *J. Am. Chem. Soc.* (submitted for publication).
Tani, T., Ohsumi, J., Mita, K., & Takiguchi, J. (1988) *J. Biol. Chem. 263*, 1231–1239.
Teshima, T., Griffin, J. C., & Powers, J. C. (1982) *J. Biol. Chem. 257*, 5085–5091.
Thompson, R. D., & Ohlsson, K. (1986) *Proc. Natl. Acad. Sci. U.S.A. 83*, 6692–6696.
Trainor, D. A. (1987) *Trends Pharmacol. Sci. 8*, 303–307.
Travis, J., & Salvesen, G. (1983) *Annu. Rev. Biochem. 52*, 655–709.
Tschesche, H., Beckmann, J., Mehlich, A., Schnabel, E., Truscheit, E., & Wenzel, H. (1987) *Biochim. Biophys. Acta 913*, 97–101.
Tsukuda, H., & Blow, D. M. (1985) *J. Mol. Biol. 184*, 703–711.
Watson, H. C., Shotton, D. M., Cox, J. C., & Muirhead, H. (1970) *Nature 225*, 806–811.
Wei, A.-Z., Mayr, I., & Bode, W. (1988) *FEBS Lett. 234*, 367–373.
Wenzel, H. R., & Tschesche, H. (1981) *Hoppe-Seyler's Z. Physiol. Chem. 362*, 829–831.
Werb, Z., Banda, M. J., McKerrow, J. H., & Sandhaus, R. A. (1982) *J. Invest. Dermatol. 79*, 154s–159s.
Williams, H. R., Lin, T.-Y., Navia, M. A., Springer, J. P., McKeever, B. M., Hoogsteen, K., & Dorn, C. P. (1987) *J. Biol. Chem. 262*, 17178–17181.
Woodbury, R. G., Katunuma, N., Kobayashi, K., Titani, K., & Neurath, H. (1978) *Biochemistry 17*, 811–819.
Yasutake, A., & Powers, J. C. (1981) *Biochemistry 20*, 3675–3679.
Zimmerman, M., & Ashe, B. M. (1977) *Biochim. Biophys. Acta 480*, 241–245.